Available online at www.sciencedirect.com
SCIENCE DIRECT®
Journal of Molecular Catalysis A: Chemical 227 (2005) 173–181
JOURNAL OF MOLECULAR CATALYSIS A: CHEMICAL
www.elsevier.com/locate/molcata

Hydro-dimerization of $Pt_2Cl_2(C_2H_4)_2$: model reaction to capture details on catalytic mechanisms

Dario Duca*

Dipartimento di Chimica Inorganica e Analitica "Stanislao Cannizzaro", Universitá di Palermo, Viale delle Scienze, Parco d'Orleans II, pad. 17, I-90128 Palermo, Sicily, Italy

Received 23 July 2004; received in revised form 7 October 2004; accepted 8 October 2004
Available online 10 December 2004

Abstract

The density functional theory was employed to mimic the homogeneous hydro-dimerization of the Zeise-similar dichloro-bis(ethene)-platinum(II), $PtCl_2(C_2H_4)_2$. Three energy minima and four transition-states were involved in the reaction mechanism, which was even characterized by a catalytic cycle.

The minima were fully optimized at B3LYP level whereas the transition-states were first individuated at the same level, by the synchronous transit-guided quasi-Newton method, then fully optimized.

The mechanistic hypotheses on the $PtCl_2(C_2H_4)_2$ dimerization implied the displacement of two ethene or two ethane molecules, respectively, occurring in absence or in presence of molecular hydrogen. In the second case, the dimer platinum product performed as a catalytic center.

The study of the reaction paths as well as that of the structural and energetic transformations of the calculated species allowed us to deepen basis aspects of the title reaction. Whereas, a comparative analysis between some species involved in the same reaction and heterogeneous catalytic models, namely ethene on platinum-cluster models, fixed some analogies between the energetics involved in homogeneous and heterogeneous catalytic processes.

Keywords: Ethene hydrogenation; Zeise derivatives; Catalysis; Kinetics; Density functional theory

1. Introduction

Recent work on heterogeneous catalysis aimed to state the occurrence of surface energy distributions able to affect the behavior of metal catalysts [1,2]. The energy sources, determining the distributions above, could be related to those assumed for the entatic enzymatic mechanisms, where the substrates locally get energy from the enzyme sites [3,4], due to local electronic and/or geometric conditions [5].

In fact, time-dependent Monte Carlo (tdMC) studies of heterogeneous catalytic systems showed that "entatic" effects, modifying the catalytic reaction rate and path, could be induced on surface processes by the available surface energy (ASE) [1,2] and by the molecule surface residence probability (Π^{ρ}) [6–10], connected to electronic and geometric conditions, respectively.

Basis quantum chemistry (qc) information [11–13] was employed within the tdMC approaches. The qc-tdMC findings seemed to confirm the possibility of developing a unique model [14,15], following first principles, able to study heterogeneous as well as homogeneous catalytic phenomena. The heuristic hypothesis of a unique model is also supported by the reported experimental difficulties in distinguishing the occurrence of homogeneous and/or heterogeneous catalytic processes [16].

To check the chance of designing a unifying "first principles" catalytic model, working at least for heterogeneous and homogeneous catalysis, the elementary steps of the title reaction were here investigated by a full computational approach and the results were compared with those, obtained at

* Tel.: +39 091 489714; fax: +39 091 427584.
E-mail address: dduca@unipa.it (D. Duca).
URL: http://www.unipa.it/dduca.

1381-1169/$ – see front matter © 2004 Elsevier B.V. All rights reserved.
doi:10.1016/j.molcata.2004.10.010

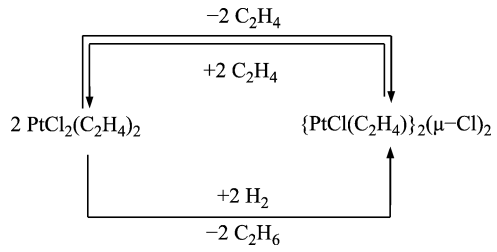

Scheme 1.

the same level, concerning simple ethene on platinum-cluster models.

The hydro-dimerization of the square planar (sp) Zeise-similar $PtCl_2(C_2H_4)_2$ species was experimentally studied in organic phase in the fifties by Flynn and Hulburlt [17]. It was pointed out that, in presence of molecular ethene and hydrogen, a minor homogeneous hydrogenation of the ethene molecules occurred at 273.15 K in acetone along with the dimerization of $PtCl_2(C_2H_4)_2$. In agreement with the work of Chatt [18], the latter species was supposed in equilibrium with the sp dichloro-bis(ethene)-(μ-dichloro)-diplatinum(II), $\{PtCl(C_2H_4)\}_2(\mu\text{-}Cl)_2$, dimer, which, in parallel, underwent systematic reduction to metallic Pt in presence of molecular hydrogen.

A competitive heterogeneous catalytic ethene hydrogenation was therefore taking place on the metallic platinum [17]. However, due to the infrequency of the homogeneous Pt hydrogenation observed at that time [17,19], very large emphasis was given to the minor homogeneous process reported in Scheme 1. The present work was focused on the process above, here indicated as FHC, because of the authors' names of the Refs. [17,18].

Five reaction steps and the catalytic hydrogenation (h) cycle of Scheme 2, were singled out. The $\{PtCl_2(C_2H_4)_2\}_2$ species is an adduct, here considered as the starting reagent, in which the single $PtCl_2(C_2H_4)_2$ fragments almost maintained the monomer structures and energetics. More details on this adduct are given in the Results and discussion section. In the catalytic cycle, S4 + f-S3 steps, ethene is hydrogenated to ethane on the dichloro-tetra(ethene)-(μ-dichloro)-diplatinum(II), $\{PtCl(C_2H_4)_2\}_2(\mu\text{-}Cl)_2$ intermediate, acting the sp $\{PtCl(C_2H_4)\}_2(\mu\text{-}Cl)_2$ species as the catalyst.

It has to be pointed that the information concerning the ethene involvement in the b-S3 and f-S3 steps, has been omitted in Schemes 2 and 3 for clearness. Moreover, since the energy of the $\{PtCl_2(C_2H_4)_2\}_2$ adduct is definitely similar to that of two isolated monomers, the two routes h0 and d of Scheme 2 individuate the FHC reaction path [17,18]. The latter is characterized by two dimerization steps, f-S1 and S5, which could take place without the involvement of intermediates.

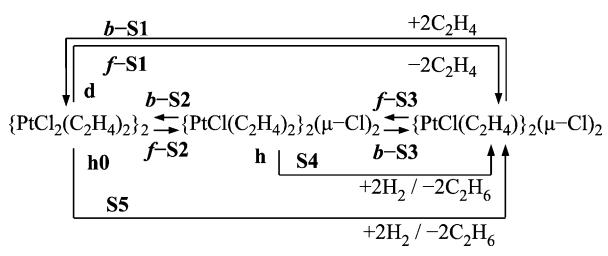

Scheme 2.

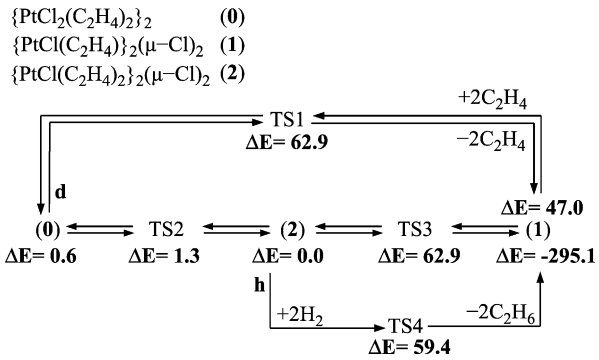

Scheme 3.

The direct S5 hydrogenation route was not considered in the present work because of the very low occurrence probability of the simultaneous collision of the four molecules needed to give rise to the corresponding transition state. Indeed, cycles h and d include also concerted molecular events. Nevertheless, these were taken into consideration, being more probable than those of S5 step.

The present qc model replicated and explained at microscopic level the complex kinetic mechanism of the title reaction [17,18]. Moreover, the calculated geometric structures of the species above were in agreement with analogous platinum molecular systems obtained following the Burdett [20] approach.

The agreement between theoretical and experimental findings, concerning the mimicking of the title hydro-dimerization path [17,18] as well as the outcomes on the structural properties [20] of the involved species, should allow us to be confident on the conclusive inference. This, also considering the results on simple heterogeneous ethene/platinum-cluster models, suggests a link at elementary level between homogeneous and heterogeneous catalysis.

2. Methods

All the calculations were performed, at the hybrid density functional B3LYP level, using the G98W package [21]. LANL2DZ [22] pseudo-potentials were employed for Pt atoms whereas the extended split-valence double-zeta 6-31G(d, p) basis set was employed for the lighter atoms.

Except for the calculation involving platinum-clusters, namely ethene on Pt_2, Pt_8 and Pt_{12} in which partial optimizations were performed imposing restraints on the relax-

ation properties of the platinum centers, molecular geometries were always fully optimized.

To speed up the optimization rate, the symmetry elements of the dimers were always considered as belonging to the C_i point group. To check the adopted approach, simpler geometries connected to the $[PtCl_3(C_2H_4)]^-$ sp anion of the Zeise salt were calculated at the same level and compared with X-ray [23] and neutron diffraction [24] crystallography findings.

Table 1 shows the good agreement between experimental and calculated results, confirming the reliability of the applied method to mimic Zeise-similar systems.

Indeed, a little disagreement arises comparing the experimental and calculated Pt–Cl distances related to the *cis*- and *trans*-chlorine atoms. Similar occurrence was observed by Bencze et al. studying at the same level of theory the structural properties of the palladium analogous, $[PdCl_3(C_2H_4)]^-$ and $[PdCl_3(C_2D_4)]^-$ anions [26]. It is likely that the systematic discrepancy found on the M–Cl distances of the calculated anionic species has to be attributed to solid state effects and/or to the absence of the K^+ counter-ion.

To test solvent and temperature effects, self-consistent reaction field (SCRF) [27] single point calculations on the in vacuo optimized structures were performed by applying the polarized continuum model [28] in the cosmo approach (CPCM) [29] of the solvent, namely acetone at 273.15 K.

Table 2 reports the energy differences in vacuo at 0 K, ΔE and ΔG°, and in solvent at 273.15 K, ΔE_{sl}, of the optimized species, detailed in the reaction path of Scheme 3, which occurs in the different reaction routes. Except for the $\{PtCl_2(C_2H_4)_2\}_2$ species the behavior of ΔE, ΔE_{sl} and ΔG° are in agreement. Noticeably, the reference ethene–ethene uncatalyzed reaction was also not affected by temperature and solvent effects.

Following the results above, as usually, only the ΔE values are considered in the following [30,31], being, in any case, confident on the effectiveness of the model employed hence on the consistence of the final conclusions.

The geometry of the transition states involved in the kinetics, both in the title hydro-dimerization and in the uncatalyzed ethene–ethene hydrogenation, were determined by employing the synchronous transit-guided quasi-Newton QST3 [32,33] method. The QST3 transition state structures were after refined by the direct TS optimization procedure within the G98W framework [21]. Following the refining procedure, minor changes in the geometries were pointed out whereas energy changes were almost absent.

The in-vacuo standard free energy values were evaluated by the thermo-chemistry analysis [27]. The harmonic vibrational analysis was also considered to check the TS attributions as well as to confirm that the stationary points were actual minima. The "loose" option was adopted in the full optimization procedure of reactants and products involving several molecular species, already singularly optimized.

A large flat potential energy region was found studying the TS species, which takes place in the S4 reduction step of Scheme 2. Indeed, few local saddle points were found, ranging within ~10 kJ mol^{-1}. To achieve these saddle points by the QST3 approach, the cut-off values of the convergence limits employed in the optimization procedures needed to be slightly increased (~0.3%) with respect to those defaulted in the G98W package [21]. The final refining TS optimization procedure did not need any cut-off value changes.

Table 1
Average distances, *d* (Å), angles, *A* (°) and dihedral angle, *D* (°) in the Zeise anion, $[PtCl_3(C_2H_4)]^-$

Structural property[a]	Calculated	X-ray[b]	NDS[c]
d(C—C)	1.40	1.37	1.38
d(C—Pt)	2.16	2.13	2.13
d(C—H)	1.09	–	1.09
A(H—C—H)[d]	117.1	–	114.9
d(Pt—$Cl_{(cis\text{-})}$)[e]	2.40	2.31	2.30
d(Pt—$Cl_{(trans\text{-})}$)	2.38	2.34	2.34
A($Cl_{(cis\text{-}1)}$—Pt—$Cl_{(cis\text{-}2)}$)	177.7	177.4	177.6
A($Cl_{(cis\text{-}1)}$—Pt—$Cl_{(trans)}$)	91.2	90.1	90.3
D(H—C—C—H)[f]	18.2	–	19.1

[a] Structures with different dihedral angle formed by the ethene plane and the Zeise molecular square plane [25] were also investigated; however, in the present work the calculated parameters of the most stable structures (both experimentally and theoretically, having the dihedral angle above ~90°) are reported.

[b] X-ray diffraction scattering data, see Ref. [23].

[c] Neutron diffraction scattering data, see Ref. [24].

[d] Average value of the angle formed between the geminal hydrogen and carbon atoms of the two —CH_2 ethene fragments.

[e] Chlorine atoms are classified with respect to the ethene fragment as *trans*- and *cis*- (*cis*-1 and *cis*-2); d (Pt—$Cl_{(cis\text{-})}$) is the average distance value between platinum and both the *cis*-1 and *cis*-2 chlorine atoms.

[f] Average dihedral angle individuated by the H—C—C—H atom arrays along the diagonals of the ethene molecular plane, showing the non planarity of the ethene fragment.

Table 2
Energy differences, ΔE (in vacuo) and ΔE_{sl} (in acetone) (kJ mol^{-1}), and standard Gibbs free energy difference, ΔG° (kJ mol^{-1}), of the species involved in given processes of the title reaction

Involved species	Process[a]	ΔE	ΔE_{sl}[b]	ΔG°
$\{PtCl_2(C_2H_4)_2\}_2$	d	0.6	0.2	−6.9
TS1	d	62.9	68.9	44.8
TS2	d	1.3	3.1	5.9
$\{PtCl(C_2H_4)_2\}_2(\mu\text{-}Cl)_2$[c]	d	0.0	0.0	0.0
TS3[d]	d|h	62.9	68.9	44.8
$\{PtCl(C_2H_4)\}_2(\mu\text{-}Cl)_2 + 2C_2H_4$	d	47.0	54.3	9.1
$\{PtCl(C_2H_4)_2\}_2(\mu\text{-}Cl)_2 + 2H_2$[c]	h	0.0	0.0	0.0
TS4	h	59.2	65.9	59.1
$\{PtCl(C_2H_4)\}_2(\mu\text{-}Cl)_2 + 2C_2H_6$	h	−295.1	−283.6	−221.7

[a] d and h show in which process, dimerization and/or hydrogenation, the species are involved.

[b] Determined at 273.15 K.

[c] $\{PtCl(C_2H_4)_2\}_2(\mu\text{-}Cl)_2$ and $\{PtCl(C_2H_4)_2\}_2(\mu\text{-}Cl)_2 + 2H_2$ are taken as reference species for the dimerization and the hydrogenation cycle, respectively.

[d] Due to the statement fixed in the note c, TS3 either in presence of hydrogen either in its absence shows the same ΔE and ΔG° values.

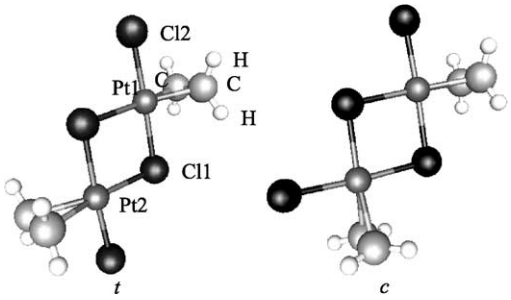

Fig. 1. Optimized structures of *trans*- (*t*) and *cis*- (*c*) $\{PtCl(C_2H_4)\}_2(\mu\text{-}Cl)_2$.

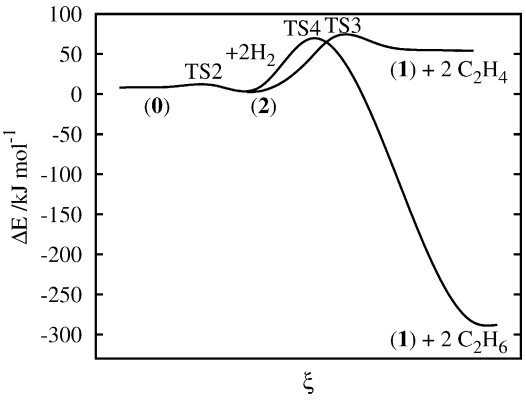

Fig. 2. Calculated energetic profiles involved in the title hydro-dimerization: ξ, reaction coordinate, (**0**) $\{PtCl_2(C_2H_4)_2\}_2$, (**1**) $\{PtCl(C_2H_4)\}_2(\mu\text{-}Cl)_2$, (**2**) $\{PtCl(C_2H_4)_2\}_2(\mu\text{-}Cl)_2$.

3. Results and discussion

The hydrogenation kinetics of the ethene fragment of the sp $[PtCl_3(C_2H_4)]^-$ anion was initially investigated to test the hypothesized catalytic properties of the platinum center in the Zeise salts [34]. Despite extensive efforts, catalytic hydrogenation routes were not found. The difficulty to find stabilized transition states in the $[PtCl_3(C_2H_4)]^-$ system is, in our opinion, determined by the presence of the negative charge and of the *trans* effect [35], both inducing the removal of the chloride ion in *trans* to the hydrocarbon, irrespective of the nature of the latter.

In order to address the kinetic study of the non-ionic FHC process to the final species without the formation of by-products, we took into account, as starting reagent, the *trans*-$PtCl_2(C_2H_4)_2$ monomer. Indeed, this species, following a nucleophilic displacement and substitution mechanism, should solely produce the *trans*-$\{PtCl(C_2H_4)\}_2(\mu\text{-}Cl)_2$ dimer. The optimized structure of this dimer with that of the *cis*-species, no considered here in the hydro-dimerization mechanism, is reported in Fig. 1. The latter shows that, irrespective of the species, the dihedral angles formed between each of the ethene planes and the molecular square plane centered on the platinum atoms are in any case almost perpendicular.

The influence of the dihedral angle above on the molecular energetics was systematically analyzed, finding that the conformers having the value of this angle close to 90° were the most stable ones. Following these evidences, here we refer only to the *trans*-species belonging to this family of conformers.

Due to the very low activation energy involved in the b-S1 as well as in the b-S2 and f-S3 steps, see Fig. 2 and Schemes 2 and 3, it is possible to hypothesize a back formation of the monomer reagents from the dimer products. In this case the sole *trans*-$PtCl_2(C_2H_4)_2$ monomer should be retro-produced.

The calculated average geometric properties and the energy difference values of the *cis*- and *trans*-$PtCl_2(C_2H_4)_2$ monomers and $\{PtCl(C_2H_4)\}_2(\mu\text{-}Cl)_2$ dimers are reported in Table 3. The table clearly shows that the choice concerning the starting reagents and the final products were supported by energetic findings. Actually, consistent trends among geometric properties of *trans*- and *cis*-monomers and dimers may not be found. However, the *trans*-species shows to be always the most stable one, taking into account the same class of compounds.

In Scheme 3 the investigated hydro-dimerization mechanism and a visual summary of the occurring energetics is reported. The ΔE values, 47.0 and -295.1 kJ mol^{-1}, concerning the $\{PtCl(C_2H_4)\}_2(\mu\text{-}Cl)_2$ plus the hydrocarbon products, arise from different energy zeros taken on the reagents of the following equations:

$$\{PtCl(C_2H_4)_2\}_2(\mu\text{-}Cl)_2 \longrightarrow \{PtCl(C_2H_4)\}_2(\mu\text{-}Cl)_2 + 2C_2H_4$$

$$\{PtCl(C_2H_4)_2\}_2(\mu\text{-}Cl)_2 + 2H_2 \longrightarrow \{PtCl(C_2H_4)\}_2(\mu\text{-}Cl)_2 + 2C_2H_6$$

Figs. 3 and 4 show the optimized structures of the minima and of the transition states, taking place in the indirect dimerization (steps f-S2 + b-S3). The single platinum fragments in the $\{PtCl_2(C_2H_4)_2\}_2$ adduct, see Section 1, maintain the sp

Table 3
Average distances *d* (Å), angles *A* (°) and energy difference ΔE (kJ mol^{-1}), characterizing *cis*- and *trans*-$PtCl_2(C_2H_4)_2$ monomer (m) and $\{PtCl(C_2H_4)\}_2(\mu\text{-}Cl)_2$ dimer (d)

Structural property[a]	*cis*-m	*trans*-m	*cis*-d	*trans*-d
d(C—C)[b]	1.39	1.38	1.40	1.41
d(C—Pt)	2.24	2.28	2.17	2.16
d(Pt1—Cl1)[c]	2.36	2.37	2.46	2.44
d(Pt1—Cl2)[c]	2.36	2.37	2.34	2.34
d(Pt2—Cl1)[d]	–	–	2.45	2.47
A(Cl1—Pt1—Cl2)[c]	90.2	180.0	177.0	177.1
A(Et—Pt—Et)[e]	90.5	180.0	–	–
ΔE[f]	15.5	0.00	6.2	0.00

[a] Structures of the monomer species are not reported. For the meaning of the atom numbering, refer to the $\{Pt(C_2H_4)Cl\}_2(\mu\text{-}Cl)_2$ species of Fig. 1.
[b] C atoms are belonging to the same ethene molecules.
[c] Chlorine and platinum atoms are belonging to the same Pt fragment.
[d] Chlorine and platinum atoms are not belonging to the same Pt fragment.
[e] The angle is obtained considering the coordinates of the mass centers of the ethene molecules belonging to one Pt fragment.
[f] *trans*-species are considered as references.

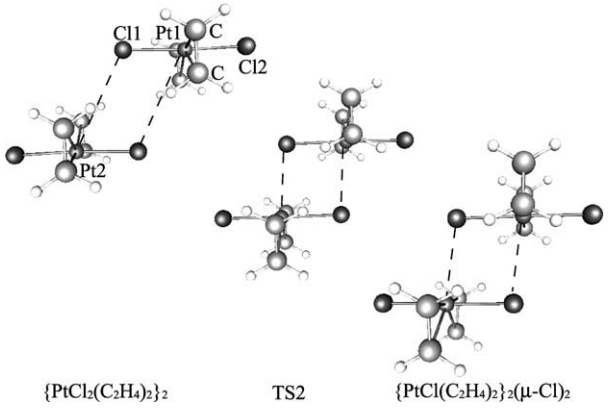

Fig. 3. Optimized structures of the species involved in the formation of the $\{PtCl(C_2H_4)_2\}_2(\mu\text{-}Cl)_2$ intermediate (f-S2 step).

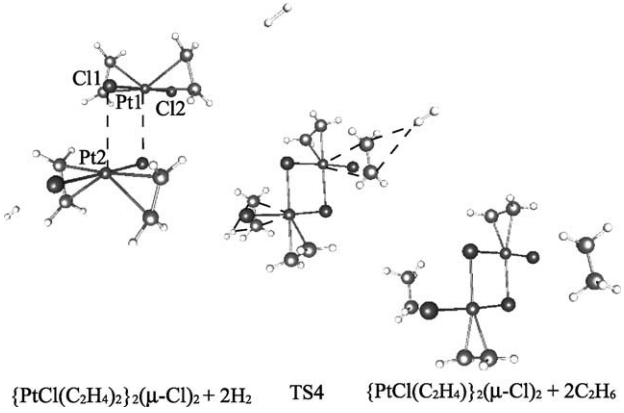

Fig. 5. Optimized structures taken into consideration along the formation of $\{PtCl(C_2H_4)\}_2(\mu\text{-}Cl)_2$, occurring by ethane displacement (S4 step).

arrangement of the $PtCl_2(C_2H_4)_2$ monomer. However, each platinum center, after the Burdett prediction [20], shows a distorted square pyramidal (spy) symmetry, which is caused by the interactions of the platinum and the chlorine centers belonging to the different monomers.

Moreover, the calculated trigonal bi-pyramidal (tbp) and sp platinum environment of the $\{PtCl(C_2H_4)_2\}_2(\mu\text{-}Cl)_2$ intermediate and $\{PtCl(C_2H_4)\}_2(\mu\text{-}Cl)_2$ product even followed the Burdett structural scheme.

Of course, the dimerization could occur without the formation of the above tbp intermediate (f-S1 step). In fact, the TS1 and TS3 geometries as well as their energies are almost equal hence both the dimerization routes could occur, in parallel, with analogous probability.

Fig. 2 and Table 2 show that the dimerization is an endothermic process. This is in agreement with the experimental findings, which show the spontaneous evolution from the dimer products to the monomer reagents in acetone at 273.15 K [36].

Fig. 5 pictures the species involved in the hydrogenation of the intermediate $\{PtCl(C_2H_4)_2\}_2(\mu\text{-}Cl)_2$ dimer. Fig. 2 and Scheme 3 point out the dramatic stabilizing effects of the hydrogenation on the dimerization products, confirming also the existence of the catalytic cycle. In fact, after the occurrence of the highly exothermic S4 hydrogenation step, the dimer product, namely the catalyst, in presence of ethene could easily back-form the intermediate $\{PtCl(C_2H_4)_2\}_2(\mu\text{-}Cl)_2$ species, following the f-S3 route.

It has here to be underlined that the latter, as highlighted by the minimum of the dotted line in Fig. 6, mimics a surface activated adsorption process, producing ethene fragments ready to be reduced in presence of hydrogen.

Fig. 6 shows the catalyzed and uncatalyzed $C_2H_4 + H_2 \longrightarrow C_2H_6$ calculated reaction profile and the involved species. It is evident the catalytic effects of the $\{PtCl(C_2H_2)\}_2(\mu\text{-}Cl)_2$ species.

Tables 4 and 5 show significant structural properties concerning the title hydro-dimerization species. As expected [20], the results of these tables point out very similar geometries for the TS2 species and the $\{PtCl(C_2H_4)_2\}_2(\mu\text{-}Cl)_2$ intermediate and, on the whole, slight changes among contiguous species along the reaction steps. Regarding the ethene frag-

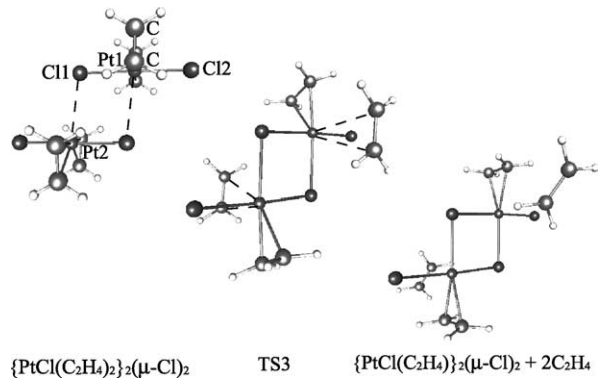

Fig. 4. Optimized structures taken into consideration along the formation of $\{PtCl(C_2H_4)\}_2(\mu\text{-}Cl)_2$, occurring by ethene displacement (b-S3 step).

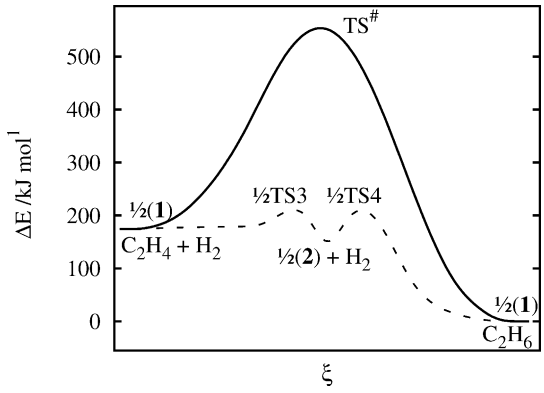

Fig. 6. Catalytic effect of $\{PtCl(C_2H_4)\}_2(\mu\text{-}Cl)_2$: (**1**), on the ethene hydrogenation through the formation of the $\{PtCl(C_2H_4)_2\}_2(\mu\text{-}Cl)_2$; (**2**), intermediate: ΔE (energy difference) vs. ξ (generalized reaction coordinate). Solid and dotted lines correspond to the calculated profile of the catalyzed and uncatalyzed C_2H_4–C_2H_6 hydrogenation, respectively. The catalyzed path follows the cycle determined by the forward and backward S3 and the S4 reaction steps.

Table 4
Ethene event identifier, $EI_{C_2H_4}$, relevant average distances d (Å) and angles A (°), characterizing different fragments of the Zeise-similar species—dimers ($\{PtCl_2(C_2H_4)_2\}_2$ (**0**), $\{PtCl(C_2H_4)\}_2(\mu\text{-}Cl)_2$ (**1**), $\{PtCl(C_2H_4)_2\}_2(\mu\text{-}Cl)_2$ (**2**)), transition states and products—involved in the dimerization cycle

Structural property[a]	$EI_{C_2H_4}$[b]	(**0**)	TS1|TS3	TS2	(**2**)	(**1**) + $2C_2H_4$
d(C—C)[c]	nl	1.38	1.42	1.39	1.39	1.41
d(C—C)[c]	og	1.38	1.35	1.39	1.39	1.34
d(C—Pt)	nl	2.27	2.14	2.25	2.25	2.16
d(C—Pt)	og	2.27	3.12	2.25	2.25	4.29
d(Pt1—Cl1)[d]	–	2.38	2.43	2.41	2.40	2.44
d(Pt1—Cl2)[d]	–	2.37	2.34	2.37	2.37	2.34
d(Pt2—Cl1)[e]	–	4.32	2.55	2.98	3.11	2.47
A(Cl1—Pt1—Cl2)[d]	–	176.9	177.4	178.7	178.8	177.0
A(Et—Pt—Et)[f]	nl | og	144.4	116.6	143.5	144.0	84.0

[a] For the meaning of the atom numbering refer to Figs. 3 and 4.
[b] nl and og characterize the considered ethene molecule: non-leaving and leaving (outgoing) the dimer, respectively.
[c] C atoms are belonging to the same ethene molecules.
[d] Chlorine and platinum atoms are belonging to the same Pt fragment.
[e] Chlorine and platinum atoms are not belonging to the same Pt fragment.
[f] Obtained considering the coordinates of the mass centers of the ethene molecules belonging to one Pt fragment, in this case one molecule is considered resident the other one leaving.

Table 5
Ethene event identifier, $EI_{C_2H_4}$, relevant average distances d (Å) and angles A (°), characterizing different fragments of the Zeise-similar species—dimers ($\{PtCl(C_2H_4)\}_2(\mu\text{-}Cl)_2$ (**1**), $\{PtCl(C_2H_4)_2\}_2(\mu\text{-}Cl)_2$ (**2**)), transition states and products—involved in the hydrogenation cycle

Structural property[a]	$EI_{C_2H_4}$[b]	(**2**)+$2H_2$	TS3	TS4	(**1**) + $2C_2H_6$
d(C—C)[c]	nl	1.39	1.42	1.42	1.41
d(C—C)[c]	og	1.39	1.35	1.39	1.53[h]
d(C—Pt)	nl	2.24	2.14	2.14	2.16
d(C—Pt)	og	2.25	3.12	3.06	4.44[h]
d(Pt1—Cl1)[d]	–	2.40	2.43	2.43	2.44
d(Pt1—Cl2)[d]	–	2.37	2.34	2.34	2.34
d(Pt2—Cl1)[e]	–	3.10	2.55	2.56	2.47
d(H—C)[f]	–	3.39	–	3.15	1.09
d(H—H)[f]	–	0.74	–	0.76	2.54
A(Cl1—Pt1—Cl2)[d]	–	178.8	177.4	177.8	177.1
A(Et—Pt—Et)[g]	nl | og	143.9	116.6	114.7	104.9[h]

[a] For the meaning of the atom numbering refer to Figs. 4 and 5.
[b] nl and og characterize the considered ethene (in the last column ethane) molecule: non-leaving and leaving (outgoing) the dimer, respectively.
[c] C atoms are belonging to the same ethene molecules.
[d] Chlorine and platinum atoms are belonging to the same Pt fragment.
[e] Chlorine and platinum atoms are not belonging to the same Pt fragment.
[f] Hydrogen atoms are those of the incoming H_2 molecules (see Fig. 5).
[g] Obtained considering the coordinates of the mass centers of the ethene molecules belonging to one Pt fragment, in this case one molecule is considered resident the other one leaving.
[h] In this column the outgoing molecules are ethane molecules.

ments, the structural effects involved in the leaving molecules of the TS1 and TS3 species are quite evident, showing the clear shortening of the C–C bond. In the TS4 transition state this feature is less evident because of the incipient transformation of ethene to ethane.

Scheme 4 shows the energy levels, characterizing hydrocarbon fragments or molecules involved in the catalyzed or uncatalyzed ethene hydrogenation. Interestingly, the starting ethene molecules show to be energized and, conversely, the transition states stabilized in the catalyzed with respect to the uncatalyzed process. This would seem to suggest that entatic effects, like those of enzymatic processes [37], could occur in the catalytic homogeneous title hydro-dimerization both on reagents and on transition states.

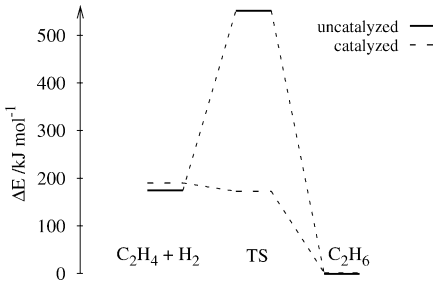

Scheme 4.

Table 6
Average distances d(C—C) (Å), angles A(H—C—H) (°), dihedral angles D(H—C—C—H) (°) and energy difference ΔE (kJ mol^{-1}), characterizing optimized ethene and ethene fragments of different species involved in the title reaction

Species[a]	d(C—C)	A(H—C—H)	D(H—C—C—H)	ΔE[b]
C_2H_4	1.34	116.4	180.0	0.0
TS$^{\#}$	1.44	109.8	105.9	296.6
$^3B_{1u(C_2H_4)}$[c]	1.53	119.1	180.0	83.4
[{PtCl(C_2H_4)$_2$}$_2$ (μ-Cl)$_2$]$_{(C_2H_4)}$	1.39	117.5	165.0	17.9
[TS4]$_{(C_2H_4)og}$	1.39	116.5	178.0	0.2
[TS4]$_{(C_2H_4)nl}$	1.42	117.6	159.1	34.7
C_2H_2/Pt_2[d]	1.50	115.0	135.8	155.9
C_2H_4/Pt_8[d]	1.49	112.3	129.7	169.7
C_2H_4/Pt_{12}[d]	1.46	114.0	136.9	114.0

[a] The geometry of the fundamental and of the first excited state of ethene, C_2H_4 and $^3B_{1u(C_2H_4)}$, and of the transition state involved in the ethane–ethane hydrogenation, TS$^{\#}$, were individually optimized, in the other cases the ethene geometries were those of the ethene fragments extracted either from the optimized dimers involved in the title reaction (species in square brackets) or from the optimized ethene metal-cluster models (C_2H_4/Pt_n): nl and og have the usual meaning (see Tables 4 and 5) whereas the energies of the extracted fragments are calculated by a single point performed at B3LYP/6-31G(d, p) level.

[b] The in vacuo ethene optimized energy is taken as zero.

[c] The calculated excitation energy value at UCIS/6-311 + G(d, p) [27] level is 364.1 kJ mol^{-1}.

[d] C_2H_4/Pt_n are considered as models of heterogeneous catalytic systems.

Table 6 shows significant structural properties and energy differences of ethene, in the fundamental and in the first excited state, and of ethene fragments involved in catalyzed, both homogeneous and heterogeneous, and uncatalyzed hydrogenation. In any case, the ethene geometry is strongly affected either by the interaction with the platinum centers either by the photo-excitation.

So, the structure of the outgoing C_2H_4 molecule of TS4 closely resembles that of the ethene minimum whereas the energy and geometry changes of the transition state involved in the uncatalyzed hydrogenation, TS$^{\#}$, are pretty different with respect to those of both homogeneous and heterogeneous catalytic transition states. Conversely, the structure of the ethene fragment in the transition states and in the metal clusters closely match (beside the dihedral angles) the ethene structure in the ethene $^3B_{1u}$ first excited state.

The catalytic structural changes, corresponding to the elongation of the C–C bond and the modifications of the H–C–H and H–C–C–H angles, suggest a progressive transformation of the valency state of the carbon atom, from 'sp^2' to 'sp^3'. This occurrence supports the hypothesis of the presence of entatic effects in the homogeneous catalysis, namely in the hydrogenation of ethene on the {PtCl(C_2H_4)$_2$}$_2$(μ-Cl)$_2$ intermediate, and suggests the existence of analogous local effects in the heterogeneous catalytic systems.

An attempt to explain the structure-reactivity relationships, pointed by the observations above, is in the following tried by analyzing the Kohn–Sham molecular orbitals [38,39], KS-MOs, of Scheme 5 where also the optimized structures of the considered species are represented under the transparencies.

The KS-HOMO$_{TS^{\#}}$, i.e. the HOMO of the optimized TS occurring in the ethene hydrogenation, is characterized by incoming H atoms (+). The KS-HOMO$_{TS^{\#}}$ shows the involvement of the ethene LUMO. A full analysis of the TS$^{\#}$ orbitals points out that the KS-HOMO$_{TS^{\#}}$ is the only MO having this property.

Therefore, the involvement of the ethene LUMO in the KS-HOMO$_{TS^{\#}}$, during the TS formation could be the cause of the energy rising along the ethene uncatalyzed hydrogenation [34].

In Scheme 5 the participation of the ethene HOMO and LUMO to occupied Kohn–Sham molecular orbitals, KS-OMOs, and specifically to the KS-HOMOs, of the {PtCl(C_2H_4)$_2$}$_2$(μ-Cl)$_2$ intermediate and of the C_2H_4/Pt_n cluster, is highlighted by dotted circles. A deep orbital analysis of the molecular systems pictured in Scheme 5 states that the represented KS-OMOs are the only showing the ethene HOMO and LUMO participation. Entatic conditions, able to affect energetics and structures occurring in catalytic hydrogenation, could be justified by the involvements of the ethene HOMO and LUMO in the OMOs of catalytic significant aggregates. This agrees, both for the homogeneous and the heterogeneous systems, with the usual organometallic compounds' description, assuming a synergism between the σ electron donation (ligand $\longrightarrow$ metal) and the π electron back-donation (metal $\longrightarrow$ ligand). In the latter, the ethene LUMO, able to raise the molecular energy, should be involved.

In fact, analogous LUMO participation, producing similar energy raising and structure changes in a given molecule, is implicitly considered in the vertical electron transition used to model excited states and was here checked for the ethene molecule by a detailed orbital analysis performed on different ethene excited states of singlet and triplet and namely in the $^3B_{1u(C_2H_4)}$.

The analysis above seems to confirm that exists a link between the energy absorption, irrespective of the nature and source of the same energy, for the ethene molecules and their geometric and orbital rearrangements. The analysis also suggests that the inclusion of the ethene LUMO in one occupied MO of a given catalytic aggregate modify the ethene geometry and, determining local energy rises, could activate the ethene displacement and transformation [34]. Indeed, the formalism above, involving localized interactions on few metallic centers, is, as already recalled, well accepted in the organometallic chemistry. However, it also finds experimental evidences in surface science. In fact, very similar heat of adsorption characterizes the interaction between small molecules, namely ethene, and different surface structures of platinum [40]. This may be explained, in the hypothesis that the molecule-surface interactions are led by local electronic and geometric, i.e. entatic, conditions just affected by the residual coordination number of single metallic centers, occurring on small site constellations.

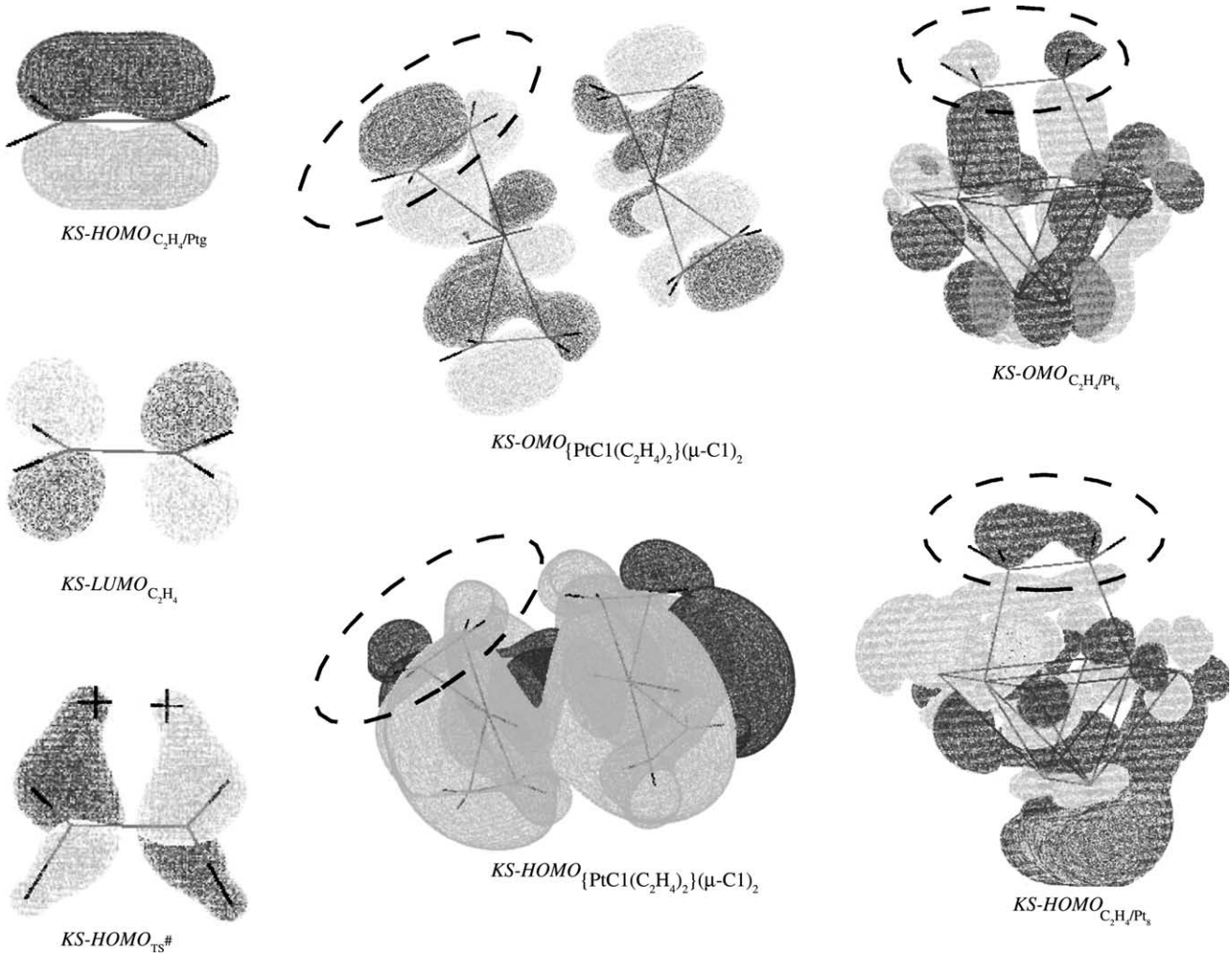

Scheme 5.

The entatic model, already used in enzymatic catalysis and here suggested to find a basis language to study heterogeneous and homogeneous processes, finally, could furnish an elementary explanation of some possible energy sources and flows, implicitly involved in the ASE [1,2] and in the Π^{ρ} [6–10] concepts, which have been previously related by stochastic approaches to local energizing effects and to molecular surface rearrangements.

4. Conclusion

The analysis of the entatic conditions, monitored by orbital rearrangements, could be employed to design new approaches and to have alternative insights in studying catalytic phenomena.

The computational approaches employed to simulate the hydro-dimerization of $PtCl_2(C_2H_4)_2$ allowed us to: (i) find out three minima and four transition states, which had geometries consistent with those predicted by the Burdett approach for analogous platinum species; (ii) replicate and detail the kinetic mechanism of the title reaction previously hypothesized on experimental bases.

Both these findings related to the structural and the kinetic properties of the species involved in the title hydro-dimerization give proof on the final inference, mainly concerning: (i) the energetics involved in catalytic transformations; (ii) a link at elementary level among catalytic processes occurring in different phases.

Acknowledgements

This work was funded by the Italian Ministero dell'Istruzione dell'Universitá e della Ricerca and by the University of Palermo.

Author thanks Prof. Vincenzo Romano, for the help given to improve the departmental computer resources; Dr. Giampaolo Barone, Dr. Antonio Prestianni and Dr. Rosario Troia for their contributions in designing and developing the

work; and Prof. Gianfranco La Manna, friend for the last two decades, for the vicennial discussions.

References

[1] D. Duca, G. La Manna, M.R. Russo, Phys. Chem. Chem. Phys 1 (1999) 1375.
[2] D. Duca, G. La Manna, Zs. Varga, T. Vidóczy, Theor. Chem. Acc. 104 (2000) 302.
[3] W. Bialek, J.N. Onuchic, Proc. Natl. Acad. Sci. USA 85 (1988) 5908.
[4] A.E. Sitnitsky, Chem. Phys. Lett. 240 (1995) 47.
[5] J.I. Steinfeld, J.S. Francisco, W.L. Hase, Chemical Kinetics and Dynamics, 2nd ed., Prentice-Hall, Upple Saddle River, NJ, 1999.
[6] D. Duca, L. Botár, T. Vidóczy, J. Catal. 162 (1996) 260.
[7] D. Duca, P. Baranyai, T. Vidóczy, J. Comp. Chem. 19 (1998) 396.
[8] D. Duca, G. Barone, Zs. Varga, Catal. Lett. 72 (2001) 17.
[9] G. Barone, D. Duca, J. Catal. 211 (2002) 296.
[10] G. Barone, D. Duca, Chem. Eng. J. 91 (2003) 139, erratum 95 (2003) 251.
[11] D. Duca, G. Barone, Zs. Varga, G. La Manna, J. Mol. Struct. (Theochem) 542 (2001) 207.
[12] G. La Manna, G. Barone, Zs. Varga, D. Duca, J. Mol. Struct. (Theochem) 548 (2001) 173.
[13] G. Barone, D. Duca, J. Mol. Struct. (Theochem) 584 (2002) 211.
[14] J.M. Basset, J.P. Candy, A. Choplin, M. Lecomte, A. Théolier, in: R. Ugo (Ed.), Aspects of Homogeneous Catalysis, vol. 7, Kluwer Academic Publishers, Dordrecht, 1990, p. 87.
[15] B.A. Averill, I.M.C.M. Rietjens, P.W.N.M. van Leeuwen, R.A. van Santen, P.W.N.M. van Leeuwen, J.A. Moulijn, B.A. Averill (Eds.), Catalysis: An Integrated Approach, Studies in Surface Sciences and Catalysis, vol. 123, 2nd ed., Elsevier, Amsterdam, 1999, p. 109.
[16] J.A. Widegren, R.G. Finke, J. Mol. Catal. A 198 (2003) 317.
[17] J.H. Flynn, H.M. Hulburt, J. Am. Chem. Soc. 76 (1954) 3493; J.H. Flynn, H.M. Hulburt, J. Am. Chem. Soc. 76 (1954) 3496.
[18] J. Chatt, Nature 165 (1950) 859; J. Chatt, J. Chem. Soc. (1952) 2622.
[19] M.L. Clarke, Polyhedron 20 (2001) 151.
[20] J.K. Burdett, Inorg. Chem. 16 (1977) 3013.
[21] M.J. Frisch, G.W. Trucks, H.B. Schlegel, G.E. Scuseria, M.A. Robb, J.R. Cheeseman, V.G. Zakrzewski, J.A. Montgomery Jr., R.E. Stratmann, J.C. Burant, S. Dapprich, J.M. Millam, A.D. Daniels, K.N. Kudin, M.C. Strain, O. Farkas, J. Tomasi, V. Barone, M. Cossi, R. Cammi, B. Mennucci, C. Pomelli, C. Adamo, S. Clifford, J. Ochterski, G.A. Petersson, P.Y. Ayala, Q. Cui, K. Morokuma, D.K. Malick, A.D. Rabuck, K. Raghavachari, J.B. Foresman, J. Cioslowski, J.V. Ortiz, A.G. Baboul, B.B. Stefanov, G. Liu, A. Liashenko, P. Piskorz, I. Komaromi, R. Gomperts, R.L. Martin, D.J. Fox, T. Keith, M.A. Al-Laham, C.Y. Peng, A. Nanayakkara, M. Challacombe, P.M.W. Gill, B. Johnson, W. Chen, M.W. Wong, J.L. Andres, C. Gonzalez, M. Head-Gordon, E.S. Replogle, J.A. Pople, Gaussian 98, Revision A.8, Gaussian, Inc., Pittsburgh, PA, 1998.
[22] P.J. Hay, W.R. Wadt, J. Chem. Phys. 82 (1985) 270.
[23] J.A.J. Jarvis, B.T. Kilbourn, P.G. Owston, Acta Cryst. B 27 (1971) 366.
[24] R.A. Love, T.F. Koetzle, G.J.B. Williams, L.C. Andrews, R. Bau, Inorg. Chem. 14 (1975) 2653.
[25] G.M. Bernard, R.E. Wasylishen, A.D. Phillips, J. Phys. Chem. A 104 (2000) 8131.
[26] É. Bencze, I. Pápai, J. Mink, P.L. Goggin, J. Organomet. Chem. 584 (1999) 118.
[27] J.B. Foresman, Æ. Frisch, Exploring Chemistry with Electronic Structure Methods, 2nd ed., Gaussian Inc., Pittsburgh, PA, 1996.
[28] V. Barone, M. Cossi, J. Tomasi, J. Comp. Chem. 19 (1998) 404.
[29] V. Barone, M. Cossi, J. Phys. Chem. A 102 (1998) 1995.
[30] M. Tlenkopatchev, S. Fomine, J. Organomet. Chem. 630 (2001) 157.
[31] D.J. Tantillo, R. Hoffmann, J. Am. Chem. Soc. 123 (2001) 9855.
[32] C. Peng, P.Y. Ayala, H.B. Schlegel, M.J. Frisch, J. Comp. Chem. 17 (1996) 49.
[33] C. Peng, H.B. Schlegel, Israel J. Chem. 34 (1994) 449.
[34] A.F. Williams, A Theoretical Approach to Inorganic Chemistry, Springer-Verlag, Berlin, 1979.
[35] G.L. Miessler, D.A. Tarr, Inorganic Chemistry, 2nd ed., Prentice-Hall, Upper Saddle River, NJ, 1998.
[36] N.N. Greenwood, A. Earnshaw, Chemistry of the Elements, 1st ed., Pergamon Press, New York, 1984.
[37] M.Y. Darensbourg, E.J. Lyon, X. Zhao, I.P. Gerorgakaki, Proc. Natl. Acad. Sci. USA 100 (7) (2003) 3683.
[38] I.N. Levine, Quantum Chemistry, 5th ed., Prentice-Hall, Upper Saddle River, NJ, 2000.
[39] E.J. Baerends, O.V. Gritsenko, J. Phys. Chem. 101 (1997) 5383.
[40] W.T. Lee, L. Ford, P. Blowers, H.L. Nigg, R.I. Masel, Surf. Sci. 416 (1998) 141.